"RHIC serves the perfect fluid" – Hydrodynamic flow of the QGP*

Ulrich Heinz

Department of Physics, The Ohio State University, Columbus, OH 43210, USA

Abstract

The bulk of the hot and dense matter created at RHIC behaves like an almost ideal fluid. I present the evidence for this and also discuss what we can learn about the transport properties of the quark-gluon plasma (QGP) from the gradual breakdown of ideal fluid dynamic behavior at large transverse momenta, lower beam energies, larger impact parameters, and forward rapidities.

1 The QCD Equation of State and ideal fluid dynamics

With relativistic heavy-ion collisions one explores the phase diagram of strongly interacting bulk matter in the regime of high energy density and temperature. Lattice QCD (LQCD) tells us [1] that for zero net baryon density QCD matter undergoes a phase transition at $T_{cr} = 173 \pm 15$ MeV from a color-confined hadron resonance gas (HG) to a color-deconfined quark-gluon plasma (QGP). The critical energy density $e_{cr} \simeq 0.7$ GeV/fm^3 [1] corresponds roughly to that in the center of a proton. At the phase transition, the normalized energy density e/T^4 rises rapidly by about an order of magnitude over a narrow temperature interval $\Delta T \lesssim 15 - 20$ MeV, whereas the pressure p/T^4 (which is proportional to the grand canonical thermodynamic potential) is continuous and rises more gradually (Fig. 1). Both seem to saturate at about 80-85% of the Stefan-Boltzmann value for an ideal gas of noninteracting quarks and gluons, the energy density more quickly (at about $1.2\,T_{cr}$), the pressure more slowly. Above about $2\,T_{cr}$, the lattice data follow the Equation of State of an ideal gas of massless particles, $e = 3p$.

For many years this observation has been interpreted as lattice QCD support for the hypothesis of a weakly interacting, perturbative QGP. The recent RHIC data taught us that this interpretation was quite wrong. The first part of the title of this talk, which was lifted from a coffee mug nowadays distributed by Brookhaven National Laboratory to their guests, alludes to this exciting discovery.

It was recognized over 3 decades ago (see review [2]) that information about the EOS of strongly
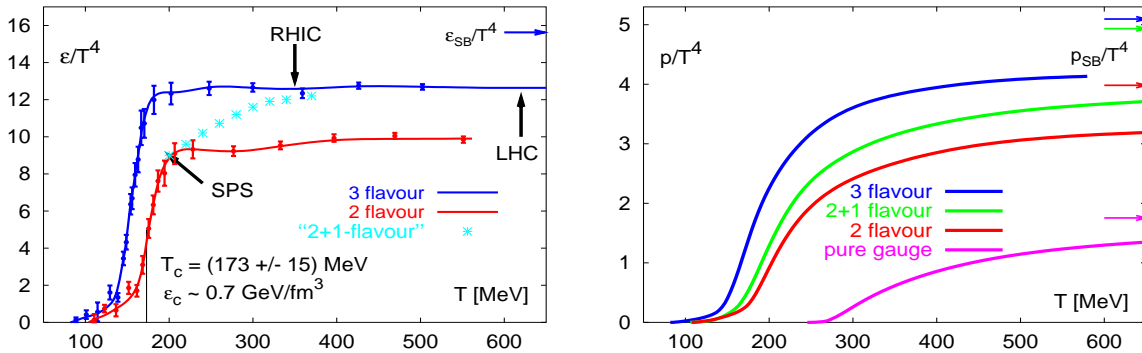

Fig. 1: The normalized energy density e/T^4 (left) and pressure p/T^4 (right) from lattice QCD [1] for 0, 2 and 3 light quark flavors, as well as for 2 light + 1 heavier (strange) quark flavors. Horizontal arrows on the right indicate the corresponding Stefan-Boltzmann values for a non-interacting quark-gluon gas.

interacting matter can be extracted by studying the collective dynamics of relativistic heavy-ion collisions. This connection is particularly direct in the framework of *ideal fluid dynamics* which becomes applicable if the matter formed in the collision approaches *local thermal equilibrium*. The latter requires

sufficiently strong interactions in the medium that local relaxation time scales are shorter than the macroscopic evolution time scale. In this limit the local conservation laws for the baryon number, energy and momentum currents, $\partial_\mu j_B^\mu(x) = 0$ and $\partial_\mu T^{\mu\nu} = 0$, can be rewritten as the relativistc Euler equations for ideal fluid motion:

$$\dot{n}_B = -n_B (\partial \cdot u), \qquad \dot{e} = -(e+p)(\partial \cdot u), \tag{1}$$

$$\dot{u}^\mu = \frac{\nabla^\mu p}{e+p} = \frac{c_s^2}{1+c_s^2} \nabla^\mu \ln\left(\frac{e}{e_0}\right). \tag{2}$$

The dot denotes the time derivative in the local fluid rest frame ($\dot{f} = u \cdot \partial f$) and ∇^μ the gradient in the directions tranverse to the fluid 4-velocity u^μ. The first line describes the dilution of baryon and energy density due to the local expansion rate $\partial \cdot u$, which itself is driven according to (2) by the pressure or energy density gradients providing the fluid acceleration. The absolute value of the energy density e is locally irrelevant: the initial maximal energy density e_0 only matters by setting the overall time scale between the beginning of hydrodynamic expansion and final decoupling, thereby controlling how much flow can develop globally. The details of the flow pattern are thus entirely controlled by the temperature dependent speed of sound $c_s^2 = \frac{\partial p}{\partial e}$.
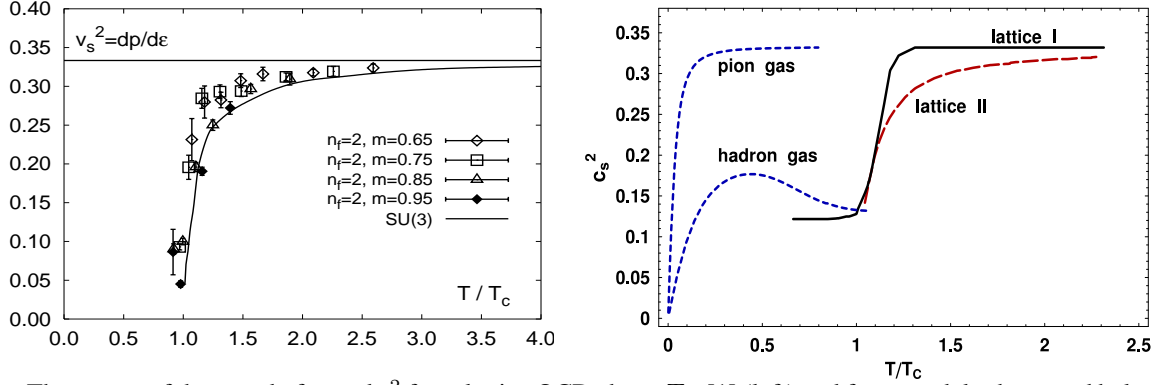

Fig. 2: The square of the speed of sound c_s^2 from lattice QCD above $T_{\rm cr}$ [1] (left) and from models above and below $T_{\rm cr}$ [3] (right).

According to the LQCD data, the latter is $c_s^2 \approx \frac{1}{3}$ for $T > 2\,T_{\rm cr}$, then drops steeply near $T \approx T_{\rm cr}$ to values near $c_s^2 \approx \frac{1}{20}$ (the "softest point", see Fig. 2, left panel), before rising again in the hadron resonance gas phase to $c_s^2 \approx 0.15$ [4] (Fig. 2, right panel). A key goal of flow studies in relativistic heavy ion collisions is to find traces of this "softest point" in the data.

2 "Flavors" of transverse flow in heavy ion collisions

Experimentally one studies flow by analyzing the transverse momentum spectra of the emitted hadrons. In central ($b=0$) collisions between spherical nuclei, the flow is azimuthally symmetric about the beam axis. This "radial flow" integrates over the entire pressure history of the collision from initial thermalization to final decoupling ("freeze-out"), due to persistent pressure gradients. In noncentral ($b \neq 0$) collisions, or central collisions between deformed nuclei such as uranium [5], the nuclear reaction zone is spatially deformed, and anisotropies of the transverse pressure gradients result in transverse flow anisotropies. These can be quantified by Fourier expanding the measured final momentum spectrum $dN/(dy\, p_\perp dp_\perp d\phi_p)$ with respect to the azimuthal angle ϕ_p. For collisions between equal nuclei, the first non-vanishing Fourier coefficient at midrapidity is the *elliptic flow* $v_2(p_\perp, b)$. Since v_2 is driven by pressure *anisotropies* and the spatial deformation of the reaction zone creating such anisotropies quickly decreases as time proceeds, the elliptic flow is sensitive to the EOS only during the early expansion stage [6] (the first ~ 5 fm/c in semicentral Au+Au collisions [7]), until the spatial deformation has disappeared.

Depending on the initial energy density (i.e. beam energy), the hot expanding fireball spends this crucial time either entirely in the QGP phase, or mostly near the quark-hadron phase transition, or

predominantly in the hadron resonance gas phase [7], thereby probing different effective values of the sound speed c_s. To the extent that ideal fluid dynamics is valid in all these cases, an excitation function of the elliptic flow v_2 should thus allow to map the temperature dependence of the speed of sound and identify the quark-hadron phase transition, via a minimum in the function $v_2(\sqrt{s})$ [7]. This will be further discussed below (see Section 5.2 and Fig. 7).

3 Model parameters and predictive power of hydrodynamics

The hydrodynamic model requires *initial conditions* at the earliest time at which the assumption of local thermal equilibrium is applicable, and a *"freeze-out prescription"* at the end when the system becomes too dilute to maintain local thermal equilibrium. Both are described in detail elsewhere [8]. Different approaches to freeze-out invoke either the Cooper-Frye algorithm [9] (used by us), in which chemical freeze-out of the hadron abundances at $T_{\rm cr}$ [10] must be implemented by hand by introducing non-equilibrium chemical potentials below $T_{\rm cr}$ [11, 12, 13], or a hybrid approach [14, 15] that switches from a hydrodynamic description to a microscopic hadron cascade at the quark-hadron transition, letting the cascade handle the chemical and thermal freeze-out kinetics. While the radial flow patterns from the two freeze-out procedures don't differ much, the elliptic flow can be quite different if the spatial deformation of the fireball is still significant during the hadronic stage of the expansion, as I will discuss in Sec. 5.2.

We have solved the relativistic equations for ideal hydrodynamics under the simplifying assumption of boost-invariant longitudinal expansion (see [7, 16] for details). This is adequate near midrapidity (the region which most RHIC experiments cover best), but not sufficient to describe the rapidity distribution of emitted hadrons and of their transverse flow pattern which require a (3+1)-dimensional hydrodynamic code such as the one by Hirano [11].

The initial and final conditions for the hydrodynamic evolution are fixed by fitting the pion and proton spectra at midrapidity in *central* collisions; additionally, we use the centrality dependence of the total charged multiplicity $dN_{\rm ch}/dy$. I stress that this is the *only* information used from $b \neq 0$ collisions, and it is necessary to fix the ratio of soft to hard collision processes in the initial entropy production. An upper limit for the initial thermalization time $\tau_0 \leq 0.6\,{\rm fm}/c$, the initial entropy density $s_0 = 110\,{\rm fm}^{-3}$ in the fireball center (corresponding to an initial peak energy density $e_0 \approx 30\,{\rm GeV/fm}^3$ and central fireball temperature $T_0 \approx 360\,{\rm MeV} \approx 2\,T_{\rm cr}$), the baryon to entropy ratio, and the freeze-out energy density $e_{\rm dec} = 0.075\,{\rm GeV/fm}^3$ are all fixed from the $b = 0$ pion and proton spectra (these numbers refer to $200\,A\,{\rm GeV}$ Au+Au collisions at RHIC [13]). The initial entropy density profile is calculated for all b from the collision geometry, using the Glauber model with soft/hard ratio as fixed above. Except for pions and protons, all other hadron spectra in $b = 0$ collisions and all spectra for $b \neq 0$ collisions (including all flow anisotropies such as v_2 which vanish at $b = 0$) are then parameter-free predictions of the model. Note that all calculated hadron spectra include feeddown from decays of unstable hadron resonances.

4 Successes of ideal fluid dynamics at RHIC

4.1 Hadron momentum spectra and radial flow

Figure 3 shows the single particle $p_\perp$-spectra for pions, kaons and antiprotons (left panel) as well as Ω baryons (right panel) measured in Au+Au collisions at RHIC, together with hydrodynamical results [13]. In order to illustrate the effect of additional radial flow generated in the late hadronic stage below $T_{\rm cr}$, two sets of curves are shown: the lower (blue) bands correspond to kinetic decoupling at $T_{\rm cr} = 165\,{\rm MeV}$, whereas the upper (red) bands assume decoupling at $T_{\rm dec} = 100\,{\rm MeV}$. The width of the bands indicates the sensitivity of the calculated spectra to an initial transverse flow of the fireball already at the time of thermalization [13]. In the hydrodynamic simulation it takes about 9-10 fm/c until most of the fireball becomes sufficiently dilute to convert to hadronic matter and another 7-8 fm/c to fully decouple [7]. Figure 3 shows that by the time of hadronization the dynamics has not yet generated enough radial flow to reproduce the measured $\bar{p}$ and Ω spectra; these heavy hadrons, which are particularly sensitive to radial flow, require the additional collective "push" created by resonant quasi-elastic interactions during the
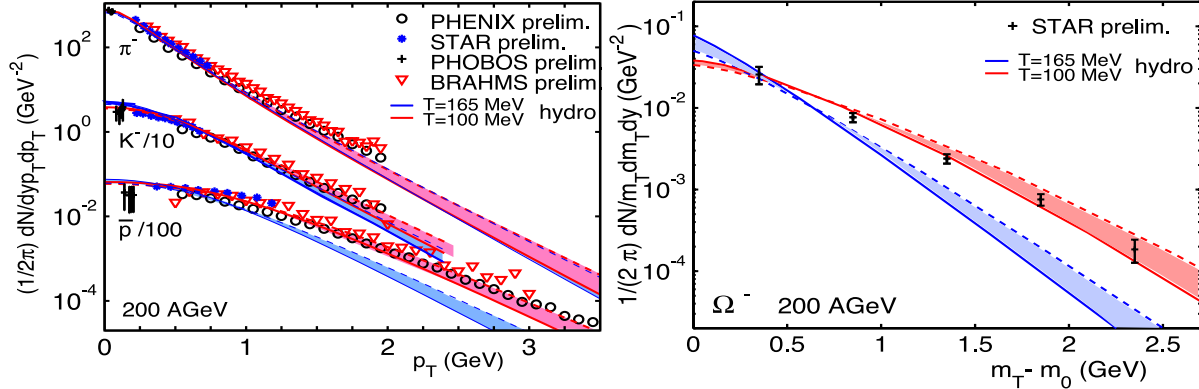
Fig. 3: Negative pion, kaon, antiproton, and Ω spectra from central Au+Au collisions at $\sqrt{s} = 200\,A\,$GeV measured at RHIC [17]. The curves show hydrodynamical calculations [13] (see text).

fairly long-lived hadronic rescattering stage. The flattening of the $\bar{p}$ spectra by radial flow provides a natural explanation for the (initially puzzling) experimental observation that for $p_\perp > 2\,$GeV/c antiprotons become more abundant than pions [16].

As shown elsewhere (see Fig. 1 in [18]), the model describes these and all other hadron spectra not only in central, but also in *peripheral* collisions, up to impact parameters of about 10 fm, and with similar quality. No additional parameters enter at non-zero impact parameter.

4.2 Elliptic flow

Figure 4 shows the predictions for the elliptic flow coefficient v_2 from Au+Au collisions at RHIC, together with the data [19, 20]. For impact parameters $b \leq 7\,$fm ($n_{\mathrm{ch}}/n_{\max} \geq 0.5$) and transverse momenta
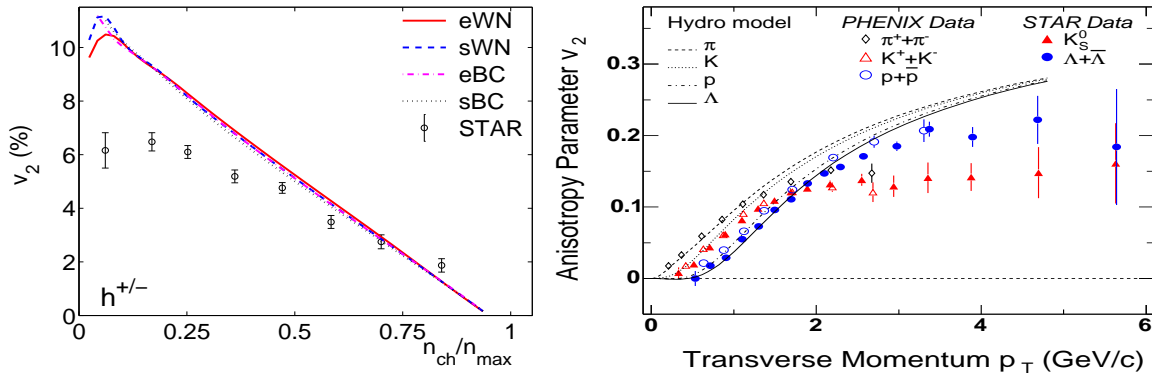

Fig. 4: Left: $p_\perp$-averaged elliptic flow for all charged hadrons from $130\,A\,$GeV Au+Au collisions, as a function of collision centrality (n_{ch} is the charged multiplicity at $y = 0$). The curves are hydrodynamic calculations with different choices for the initial energy density profile (see [21]). Right: Differential elliptic flow $v_2(p_\perp)$ for identified hadrons from minimum bias Au+Au collisions at $200\,A\,$GeV [19, 20, 22], together with hydrodynamic curves from [23].

$p_\perp \lesssim 1.5\,$GeV/c the data are seen (left panel of Fig. 4) to exhaust the upper limit for v_2 obtained from the hydrodynamic calculations. For larger impact parameters $b > 7\,$fm the $p_\perp$-averaged elliptic flow v_2 increasingly lags behind the hydrodynamic prediction; this will be discussed in detail in Sec. 5.2. As a function of $p_\perp$ (right panel of Fig. 4) the elliptic flow of all hadrons measured so far is very well described by hydrodynamics, for $p_\perp \lesssim 1.5 - 2\,$GeV/$c$. In particular the hydrodynamically predicted *mass splitting* of v_2 at low $p_\perp$ is perfectly reproduced by the data. This mass splitting depends on the EOS [23], and the EOS including a quark-hadron phase transition used here describes the data better than one without phase transition (see Fig. 2 in [18]). Ideal fluid dynamics with a QGP EOS thus gives an excellent and very detailed description of *all* hadron spectra below $p_\perp = 1.5\,$GeV/c. Since this $p_\perp$-range includes more

than 99% of all produced hadrons, it is fair to say that *the bulk of the fireball matter formed in Au+Au collisions at RHIC behaves very much like a perfect fluid.*

4.3 Final source eccentricity in coordinate space

While spectra and elliptic flow reflect the *momentum* structure of the hadron emitting source, its *spatial* deformation can be tested with 2-pion Hanbury Brown-Twiss (HBT) correlations measured as a function of the azimuthal emission angle [24, 25]. Even though the initial spatial deformation of the reaction zone in non-central Au+Au collisions at RHIC is finally completely gone, many pions are already emitted from earlier times when the spatial deformation is still significant. For Au+Au collisions at $b = 7$ fm, the spatial eccentricity of the time-integrated hydrodynamic pion emission function is $\langle \varepsilon_x \rangle = 0.14$ (or 56% of its initial value $\varepsilon_x(\tau_0) = 0.25$) [24]. Using azimuthally sensitive pion HBT measurements, the STAR Collaboration has measured in the corresponding impact parameter bin [26] $\langle \varepsilon_x \rangle = 0.11, \pm 0.035$ (or $45 \pm 15\%$ of the initial deformation). This can be counted as another success for hydrodynamics.

5 Viscous effects at RHIC

5.1 QGP viscosity

As evident in the right panel of Fig. 4, the hydrodynamic prediction for $v_2(p_\perp)$ gradually breaks down above $p_\perp \gtrsim 1.5$ GeV/c for mesons and above $p_\perp \gtrsim 2.2$ GeV/c for baryons. The empirical fact [22] that both the $p_\perp$-values, where this break from hydrodynamics sets in, and the saturation values for v_2 at high $p_\perp$ for baryons and mesons are always (*i.e. for all collision centralities!*) related by 3:2 (i.e. by their ratios of valence quark numbers), independent of their masses, tells its own interesting story (see e.g. [27]): It strongly suggests that in this $p_\perp$ region hadrons are formed by coalescence of color-deconfined quarks, and that the elliptic flow is of partonic origin (i.e. generated before hadronization), with a $p_\perp$-shape that follows hydrodynamics at low $p_\perp$ up to about 750 MeV and then gradually breaks away [27].

Since $v_2(p_\perp)$ is a measure for the relatively small differences between the in-plane and out-of-plane slopes of the $p_\perp$ spectra, it is more sensitive to deviations from ideal fluid dynamic behaviour than the angle-averaged slopes. Two model studies [28, 29] showed that v_2 reacts particularly strongly to shear viscosity. As the mean free path of the plasma constituents (and thus the fluid's viscosity) goes to zero, v_2 approaches the ideal fluid limit from below [30] (see Fig. 5a). At higher transverse momenta it does so more slowly than at low $p_\perp$ [30], approaching a constant saturation value at high $p_\perp$. The increasing deviation from the ideal fluid limit for growing $p_\perp$ is qualitatively consistent with the expected influence
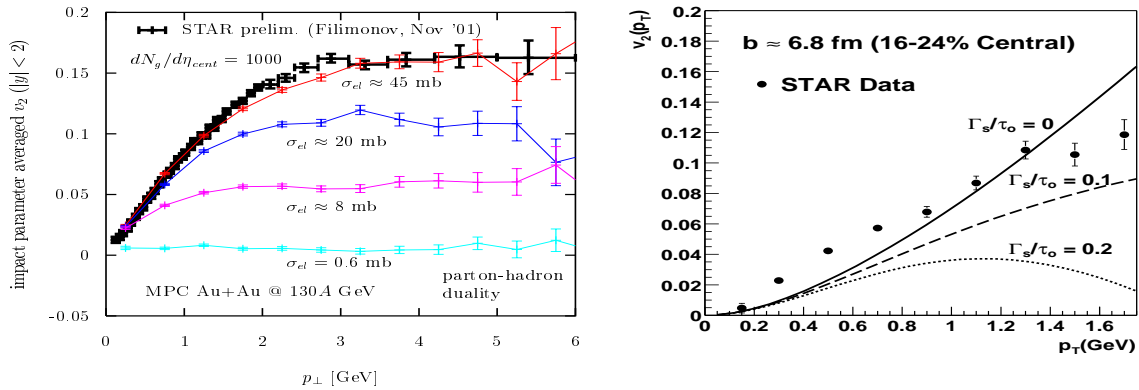

Fig. 5: Left: Elliptic flow from a parton cascade [30], compared with STAR data, for different parton-parton scattering cross sections. Larger cross sections lead to smaller mean free paths. Right: Perturbative effects of shear viscosity on the elliptic flow $v_2(p_\perp)$ [29] (see text).

of shear viscosity: Teaney [29] showed that the lowest order viscous corrections to the local equilibrium distribution increase quadratically with $p_\perp$ so that v_2 remains increasingly below the ideal fluid limit as $p_\perp$ grows (see Fig. 4b). From Fig. 5b Teaney concluded that at RHIC the normalized sound attenuation

length $\frac{\Gamma_s}{\tau} = \frac{4}{3T\tau}\frac{\eta}{s}$ (where η is the shear viscosity, T the temperature and s the entropy density) cannot be much larger than about 0.1. This puts a stringent limit on the dimensionless ratio η/s, bringing it close to the recently conjectured absolute lower limit for the viscosity of $\eta/s = \hbar/(4\pi)$ [31]. This would make the quark-gluon plasma the most ideal fluid ever observed [31].

These arguments show that deviations from ideal fluid dynamics at high $p_\perp$ must be expected, and that they can be large even for fluids with very low viscosity. At which $p_\perp$ non-ideal effects begin to become visible in $v_2(p_\perp)$ can be taken as a measure for the fluid's viscosity. To answer the *quantitative* question what the RHIC data on partonic elliptic flow and its increasing deviation from ideal fluid behaviour above $p_\perp \gtrsim 750\,\mathrm{MeV}/c$ imply for the *value* of the QGP shear viscosity η requires a numerical algorithm for solving viscous relativistic hydrodynamics, see [32].

5.2   Viscosity of the hadron resonance gas

Ideal fluid dynamics also fails to describe the elliptic flow v_2 in more peripheral Au+Au collisions at RHIC and in central and peripheral collisions at lower energies (see Fig. 6a), as well as at forward rapidities in minimum bias Au+Au collisions at RHIC [33]. Whereas hydrodynamics predicts a non-monotonic beam energy dependence of v_2 (Fig. 7a [7]), with largest values at upper AGS and lower SPS energies, somewhat lower values at RHIC and again larger values at the LHC, the data seem to increase monotonically with $\sqrt{s}$.
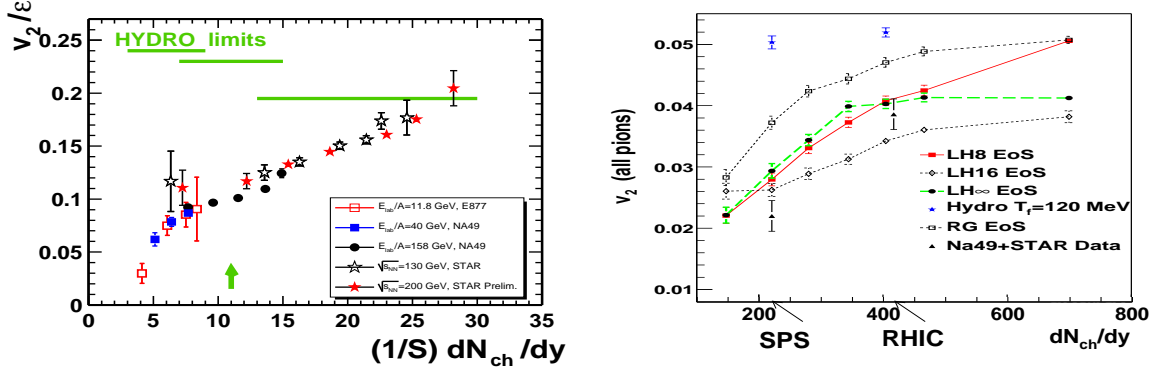

Fig. 6: Left: Scaled elliptic flow v_2/ε (ε denotes the initial spatial eccentricity) vs. the charged multiplicity per unit initial transverse overlap area S [34]. Right: Elliptic flow v_2 for minimum bias Au+Au collisions at various collision energies, parametrized by the final charged multiplicity density at midrapidity [15].

Such a monotonic rise is consistent with "hybrid" calculations by Teaney [15] (Fig. 6b) where the fireball undergoes ideal fluid dynamic evolution only while in the QGP, followed by hadronic *kinetic* evolution using RQMD after hadronization. Figure 6b shows several curves corresponding to different equations of state during the hydrodynamic evolution (see [15]), with LH8 being closest to the lattice data. The difference between the points labelled LH8 and the hydrodynamic values at the top of the figure is due to the different evolution during the late hadronic stage. Obviously, at lower collision energies and for impact parameters $b \sim 7\,\mathrm{fm}$ (simulating minimum bias collisions), ideal fluid dynamics continues to build additional elliptic flow during the hadronic stage, but RQMD does not. The initial energy densities are smaller than at RHIC and the fireball does not spend enough time in the QGP phase for the spatial eccentricity ε to fully relax before entering the hadron resonance gas phase. Anisotropic pressure gradients thus still exist in the hadronic phase, and ideal fluid dynamics reacts to them according to the stiffness of the hadron resonance gas EOS ($p \approx 0.15e$). Teaney's calculations [15] show that RQMD responds to these remaining anisotropies much more weakly, building very little if any additional elliptic flow during the hadronic phase. The hadron resonance gas is a highly viscous medium, unable to maintain local thermal equilibrium. The failure of the hydrodynamic model in situations where the initial energy density is less than about $10\,\mathrm{GeV/fm^3}$ [35] is therefore likely *not* the result of viscous effects in the early QGP fluid, but rather caused by the highly viscous late hadronic stage which is unable to efficiently

respond to any remaining spatial deformation. This is supported by a compilation of midrapity data on single particle spectra and elliptic flow as a function for $p_\perp$ for pions and protons by the PHENIX Collaboration (Fig. 20 in [36]) which shows that (i) no purely ideal fluid dynamic model can describe all the data, (ii) differences among theories and between theoretical predictions and the experimental data can all be traced to different ways of describing the *hadronic* stage of the expansion, and (iii) the only model which describes all data simultaneously is the hybrid hydro+cascade approach by Teaney et al. [15].

   Similar arguments hold at forward rapidities at RHIC [35] where the initial energy densities are also significantly smaller than at midrapidity while the initial spatial eccentricities are similar. We recently performed an analysis of the rapidity dependence of the charged hadron elliptic flow [37] for different collision centralities within a hybrid hydro+cascade approach [38] and found that, at least with the standard Glauber model initial conditions, hadronic dissipation in the late hadron resonance gas stage can fully explain the deviations between data and ideal fluid dynamics at forward rapidities and in peripheral collisions. Some additional QGP viscosity may be needed if the initial state is instead controlled by gluon saturation (see [38] for details).

5.3   Where is the phase transition signature?

The large hadron gas viscosity spoils one of the clearest experimental signatures for the quark-hadron phase transition, the predicted [7] non-monotonic beam energy dependence of v_2 which was already described in Sec. 2 and is shown in Fig. 7a. As one comes down from infinite beam energy, v_2 is predicted to first decrease (due to the softening of the EOS in the phase transition region) and then recover somewhat in the moderately stiff hadron gas phase. The hadron gas viscosity spoils this recovery,
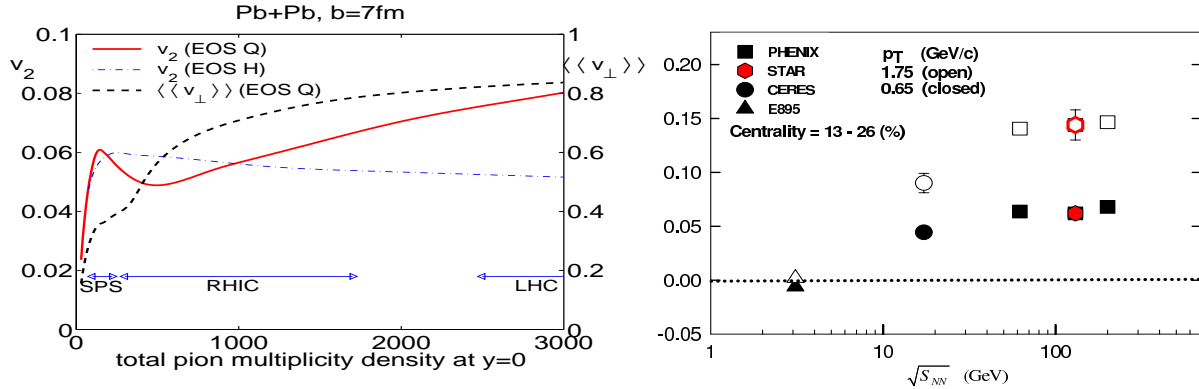

Fig. 7: Left: Excitation function of radial and $p_\perp$-integrated elliptic flow for $b = 7$ fm Pb+Pb or Au+Au collisions [7]. The horizontal axis gives $dN_\pi/dy(b{=}7\,\text{fm})$, and the horizontal arrows indicate how dN_π/dy was expected to correspond to the beam energy ranges covered by SPS, RHIC and LHC before the RHIC data were available. Right: Elliptic flow at fixed $p_\perp = 0.65$ and $1.75\,\text{GeV}/c$ from A+A collisions with $A \approx 200$ at a variety of beam energies [40].

leading to an apparently monotonous decrease of v_2 with falling beam energy (Fig. 6). However, recent PHENIX data from Au+Au collisions at $\sqrt{s} = 62\,A$ GeV [40] indicate that this decrease may not be quite as monotonous as suggested by Fig. 6a. Figure 7b shows that, at fixed $p_\perp$, the elliptic flow $v_2(p_\perp)$ is essentially constant over the entire energy range explored at RHIC (from 62 to 200 A GeV), decreasing only when going further down to SPS and AGS energies. When integrated over $p_\perp$, this turns into a monotonous behaviour as in Fig. 6a, due to the steepening $p_\perp$ spectra at lower $\sqrt{s}$. While Fig. 7b does not confirm the hydrodynamically predicted *rise* of v_2 towards lower $\sqrt{s}$, it may still reflect this predicted non-monotonic structure in the elliptic flow excitation function, after strong dilution by hadronic viscosity effects [38, 39]. Obviously, many and more systematic hybrid calculations of the type pioneered by Teaney [15] are necessary to explore to what extent we can eventually prove the existence of a QCD phase transition using elliptic flow data in the SPS-RHIC energy domain.

Obviously, it will be important to confirm non-viscous fluid behaviour at higher initial energy densities than so far explored, by extending Fig. 6a to the right and verifying that v_2/ε settles on the hydrodynamic curve. This can be done with Pb+Pb collisions at the LHC, or with full-overlap U+U collisions at RHIC [5]. In addition, the large spatial source deformations achievable in full-overlap side-on-side U+U collisions allow for decisive systematic studies of the non-linear path-length dependence of QCD radiative energy loss of fast partons. In [5] we give quantitative arguments why a U+U collision program should be seriously considered at RHIC.

5.4 Reconstructing the total momentum anisotropy from hadron data

As discussed above in Section 5.2, no purely hydrodynamic model is able to simultaneously reproduce all low-$p_\perp$ RHIC data, and (at the very least) some hadronic viscosity, implemented through a realistic hadronic cascade for the late expansion stage, must be considered. But if the observed hadron spectra and elliptic flow depend on the details of the late hadronic evolution [41], doesn't this invalidate the claim that the momentum anisotropy is created early and probes the EOS of the hot QGP stage?

The answer to this critical question is: "No, but . . . ." Once the initial spatial eccentricity is gone, there is no further driving force for additional momentum anisotropy, and the only thing that can happen henceforth is that the latter is redistributed among the various hadron species and in transverse momentum [41]. If the total momentum anisotropy saturates before the system hadronizes, hadronic viscosity is no problem for the overall momentum anisotropy (which is then entirely controlled by the preceding QGP and its EOS), and it can be fully reconstructed from the measured hadron spectra. However, the flow measure to look at for this purpose is not v_2, but instead the $p_\perp^2$-weighted elliptic flow [42]. Using the kinetic theory relation $T^{\mu\nu}(x) = \sum_i \int (d^3p/E) p^\mu p^\nu f_i(x,p)$ we can express the total final momentum anisotropy as a sum over contributions from all hadron species:

$$\epsilon_p^{\text{final}} = \frac{\langle T^{xx} - T^{yy}\rangle_{\Sigma_{\text{f}}}}{\langle T^{xx} + T^{yy}\rangle_{\Sigma_{\text{f}}}} = \frac{\sum_{i\in\text{hadrons}} \int p_\perp^2 \cos(2\phi_p) \frac{dN_i}{dy\, p_\perp dp_\perp\, d\phi_p}\, d^2p_\perp}{\sum_{i\in\text{hadrons}} \int p_\perp^2 \frac{dN_i}{dy\, p_\perp dp_\perp\, d\phi_p}\, d^2p_\perp} \tag{3}$$

Here $\langle \ldots \rangle_{\Sigma_{\text{f}}}$ denotes an integral over the final kinetic decoupling hypersurface. Note that this expression is not entirely model-independent since it requires correcting the measured hadron spectra for post-freezeout resonance decays.

For ideal fluids which live long enough for the spatial eccentricity to vanish and hence the momentum anisotropy to saturate before the hadrons decouple, this $\epsilon_p^{\text{final}}$ is a clean probe of the (time- and temperature-averaged) speed of sound of the dense matter, as discussed in Section 1. However, if the QGP hadronizes before ϵ_p saturates (i.e. if the system enters the hadronic stage with significant spatial eccentricity left over), $\epsilon_p^{\text{final}}$ becomes sensitive to large dissipative effects during the late hadronic stage. This dilutes and distorts its sensitivity to the softening of the EOS (dropping speed of sound) during the quark-hadron phase transition, as discussed in the preceding subsection. An assessment of the remaining sensitivity of the excitation function (i.e. beam energy dependence) of $\epsilon_p^{\text{final}}$ to the quark-hadron transition and its usefulness as a phase transition signature [7, 39] thus requires systematic quantitative studies of the time evolution of ϵ_p within hydro+cascade hybrid models such as those used in [15, 38].

6 Ideal fluid response of the QGP to penetrating hard partons

If the QGP indeed behaves as an almost perfect fluid, an interesting issue are possible hydrodynamic effects caused by jet quenching, i.e. by the localized energy deposited by a fast parton created early in the collision as it propagates through the dense fireball, colliding with the plasma constituents and radiating gluons [43]. Due to space limitations I can only give a very abbreviated discussion here of this exciting question. There is experimental evidence [44] that the energy lost by fast partons traveling through the dense QCD medium formed in Au+Au collisions at RHIC largely thermalizes. Since the source of this deposited energy, the fast parton, travels at supersonic speed, it was suggested that this should generate either a hydrodynamic conical Mach shock wave propagating through the ideal QGP

fluid [45] or a conical colored wake field propagating through the quark-gluon plasma [46, 47]. In either case, it was expected [45, 46, 47] that this should lead to anisotropic particle emission along a cone around the direction of the fast parton whose opening angle would reflect the speed of sound or the speed of collective plasma waves (both important plasma properties) in the quark-gluon plasma.

A lot of excitement was generated by the fact that the PHENIX Collaboration [48] saw structures in the angular correlations of hadron emission relative to the direction of a fast trigger particle which might be evidence for such conical flow. The STAR Collaboration, on the other hand, did not see clear conical structures, but only a general broadening of the peak associated with the direction of the quenching jet [44, 49]. A recent hydrodynamical simulation [50] showed that conical flow generated by the fast parton and superimposed on the radial expansion flow of the fluid is indeed visible in the calculation, but that (even under the optimized conditions studied in [50]) it does not manifest itself through the predicted peaks in the angular distribution of emitted hadrons. Other hydrodynamic effects, such as local heating and backsplash from the "crater" created by the fast parton, overlay the Mach cone phenomenon, the final result only being a large broadening of the peak associated with the quenching jet [50].

7 Conclusions

The collective flow patterns observed at RHIC provide strong evidence for fast thermalization at less than $1\,\mathrm{fm}/c$ after impact and at energy densities more than an order of magnitude above the critical value for color deconfinement. The thus created thermalized QGP is a strongly coupled plasma which behaves like an almost ideal fluid. These features are first brought out in heavy-ion collisions at RHIC near midrapidity because only there the initial energy densities and QGP life times are large enough for the ideal fluid character of the QGP to really manifest itself, in the form of fully saturated hydrodynamic elliptic flow, undiluted by late non-equilibrium effects from the highly viscous hadron resonance gas which dominates the expansion at lower energies.

We are now ready for a systematic experimental and theoretical program to quantitatively extract the EOS, thermalization time and transport properties of QGP and hot hadronic matter. This requires more statistics and a wider systematic range for soft hadron production data, but more importantly a wide range of systematic simulation studies with the "hydro-hadro" hybrid algorithms and, above all, a (3+1)-dimensional viscous relativistic hydrodynamic code (see [32] for more on that).

References

[1] F. Karsch and E. Laermann, in *Quark-Gluon Plasma 3*, edited by R. C. Hwa and X.-N. Wang (World Scientific, Singapore, 2004), p. 1 [arXiv:hep-lat/0305025].

[2] H. Stöcker and W. Greiner, *Phys. Rept.* **137** (1986) 277.

[3] M. Chojnacki, W. Florkowski and T. Csörgő, Phys. Rev. C **71** (2005) 044902.

[4] J. Sollfrank *et al.*, Phys. Rev. C **55** (1997) 392

[5] U. Heinz and A. J. Kuhlman, Phys. Rev. Lett. **94** (2005) 132301; A. J. Kuhlman and U. Heinz, Phys. Rev. C **72** (2005) 037901.

[6] H. Sorge, Phys. Rev. Lett. **78** (1997) 2309.

[7] P. F. Kolb, J. Sollfrank and U. Heinz, Phys. Rev. C **62** (2000) 054909.

[8] U. Heinz, AIP Conf. Proc. **739** (2004) 163.

[9] F. Cooper and G. Frye, Phys. Rev. D **10** (1974) 186.

[10] P. Braun-Munzinger, D. Magestro, K. Redlich and J. Stachel, Phys. Lett. B **518** (2001) 41.

[11] T. Hirano and K. Tsuda, Phys. Rev. C **66** (2002) 054905.

[12] R. Rapp, Phys. Rev. C **66** (2002) 017901; D. Teaney, Phys. Rev. C **61** (2001) 006409.

[13] P. F. Kolb and R. Rapp, Phys. Rev. C **67** (2003) 044903.

[14] S. A. Bass and A. Dumitru, Phys. Rev. C **61** (2000) 064909.

[15] Teaney D, Lauret J and Shuryak E V 2001 Phys. Rev. Lett. **86** 4783, and *Preprint* nucl-th/0110037.

[16] P. F. Kolb and U. Heinz, in *Quark-Gluon Plasma 3*, edited by R. C. Hwa and X.-N. Wang (World Scientific, Singapore, 2004), p. 634 [arXiv:nucl-th/0305084].

[17] T. Chujo *et al.*[PHENIX Collaboration], Nucl. Phys. **A715** (2003) 151c; O. Barannikova, F. Wang *et al.*[STAR Collaboration], Nucl. Phys. **A715** (2003) 458c; B. Wosiek *et al.*[PHOBOS Collaboration], Nucl. Phys. **A715** (2003) 510c; D. Ouerdane *et al.*[BRAHMS Collaboration], Nucl. Phys. **A715** (2003) 478c; C. Suire *et al.*[STAR Collaboration], Nucl. Phys. **A715** (2003) 470c.

[18] U. Heinz and P. F. Kolb, in *Proc. 18th Winter Workshop on Nuclear Dynamics*, edited by R. Bellwied *et al.*(EP Systema, Debrecen, Hungary, 2002), p.205 [arXiv:hep-ph/0204061].

[19] K. H. Ackermann K H *et al.*[STAR Collaboration], Phys. Rev. Lett. **86** (2001) 402; C. Adler *et al.*[STAR Collaboration], Phys. Rev. Lett. **87** (2001) 182301; Phys. Rev. Lett. **89** (2002) 132301; Phys. Rev. C **66** (2002) 034904; Phys. Rev. Lett. **90** (2003) 032301; J. Adams *et al.*[STAR Collaboration], Phys. Rev. Lett. **92** (2004) 052302.

[20] K. Adcox *et al.*[PHENIX Collaboration], Phys. Rev. Lett. **89** (2002) 212301; S. S. Adler *et al.*[PHENIX Collaboration], Phys. Rev. Lett. **91** (2003) 182301.

[21] P. F. Kolb, U. Heinz, P. Huovinen, K. J. Eskola and K. Tuominen, Nucl. Phys. **A696** (2001) 175.

[22] P. R. Sorensen, Ph.D. thesis (2003) [arXiv:nucl-ex/0309003].

[23] P. Huovinen, P. Kolb, U. Heinz, P. V. Ruuskanen and S. A. Voloshin, Phys. Lett. B **503** (2001) 58.

[24] U. Heinz and P. F. Kolb, Phys. Lett. B **542** (2002) 216.

[25] F. Retière and M. A. Lisa, Phys. Rev. C **70** (2004) 044907.

[26] J. Adams *et al.*[STAR Collaboration], Phys. Rev. Lett. **93** (2004) 012301.

[27] B. Müller, Nucl. Phys. **A750** (2005) 84; D. Molnar and S. A. Voloshin, Phys. Rev. Lett. **91** (2003) 092301.

[28] U. Heinz and S. M. H. Wong, Phys. Rev. C **66** (2002) 014907.

[29] D. Teaney, Phys. Rev. C **68** (2003) 034913, and private communication.

[30] D. Molnar and M. Gyulassy, Nucl. Phys. **A697** (2002) 495. (Erratum *ibid.* **A703** (2002) 893);

[31] P. Kovtun, D. T. Son and A. O. Starinets, Phys. Rev. Lett. **94** (2005) 111601.

[32] A. K. Chaudhuri and U. Heinz, arXiv:nucl-th/0504022; U. Heinz, these proceedings.

[33] T. Hirano, Phys. Rev. C **65** (2002) 011901.

[34] C. Alt *et al.*[NA49 Collaboration], Phys. Rev. C **68** (2003) 034903.

[35] U. Heinz and P. F. Kolb, J. Phys. G **30** (2004) S1229.

[36] S. S. Adler *et al.*[PHENIX Collaboration], Nucl. Phys. **A757** (2005) 184.

[37] B. B. Back *et al.*[PHOBOS Collaboration], Phys. Rev. C **72** (2005) 051901(R).

[38] T. Hirano, U. Heinz, D. Kharzeev, R. Lacey and Y. Nara, arXiv:nucl-th/0511046.

[39] H. Sorge, Phys. Rev. Lett. **82** (1999) 2048.

[40] S. S. Adler *et al.*[PHENIX Collaboration], Phys. Rev. Lett. **94** (2005) 232302.

[41] This is even true in purely hydrodynamic simulations, if one changes the hadronic equation of state, e.g., by implementing earlier chemical than kinetic freeze-out, see T. Hirano and M. Gyulassy, arXiv:nucl-th/0506049, and [13]. These authors showed that different chemical compositions of the hadronic phase cause the overall momentum anisotropy to be distributed differently both in $p_\perp$ and among the various hadronic species, even after all spatial anisotropies of the pressure gradients have disappeared and hence the total momentum anisotropy has fully saturated.

[42] J. Y. Ollitrault, Phys. Rev. D **46** (1992) 229.

[43] M. Gyulassy, I. Vitev, X. N. Wang and B. W. Zhang, in *Quark-Gluon Plasma 3*, edited by R. C. Hwa and X.-N. Wang (World Scientific, Singapore, 2004), p. 123 [arXiv:nucl-th/0302077].

[44] J. Adams *et al.* [STAR Collaboration], Phys. Rev. Lett. **95** (2005) 152301.

[45] J. Casalderrey-Solana, E. V. Shuryak and D. Teaney, hep-ph/0411315.

[46] H. Stöcker, Nucl. Phys. A **750** (2005) 121.

[47] J. Ruppert and B. Müller, Phys. Lett. B **618** (2005) 123.

[48] S. S. Adler *et al.* [PHENIX Collaboration], nucl-ex/0507004.

[49] J. G. Ulery [STAR Collaboration], arXiv:nucl-ex/0510055.

[50] A. K. Chaudhuri and U. Heinz, arXiv:nucl-th/0503028 (v3).